Progress In Electromagnetics Research C, Vol. 131, 197–208, 2023

Design and Development of a Miniaturized Highly Isolated UWB-MIMO Diversity Antenna with Quad Band Notch Characteristics

Sadineni Ramesh Babu[1, *] and Puttaraje Dinesha[2]

Abstract—A miniaturized quadruple band reject UWB-MIMO antenna with high degree of isolation is designed and experimentally evaluated in this study. The reported design utilizes dual antenna elements that are organized orthogonally by employing polarization diversity. Notch bands can be acquired by incorporating three U-shape slots and a split ring resonator (SRR) on the antenna element that exhibits band rejection of 3.41–4.07 GHz, 4.41–4.76 GHz, 5.21–5.64 GHz, and 6.92–8.63 GHz to reject the potential interference from 5G, INSAT, WLAN, and X-band. The UWB-MIMO antenna is resonating in the frequency band from 2.9 to 12 GHz with a good isolation (< -25 dB). The response of the reported antenna has been examined experimentally in terms of notch frequencies, surface current variation, gain, radiation patterns, envelope correlation coefficient, diversity gain, and total active reflection coefficient.

1. INTRODUCTION

In 2002, the Federal Communications Commission (FCC) authorized the use of ultra-wideband (UWB) frequencies between 3.1 and 10.6 GHz, initially for radar systems but later for data transmissions due to its high data rates and channel capacity [1]. UWB antennas, however, are afflicted by multi-route fading [2]. When UWB is used in tandem with multiple-input multiple-output (MIMO) antenna technology, not only is transmission capacity and dependability increased, but multi-path fading is also mitigated [3]. Multiple-input, multiple-output improves reliability by employing numerous antennas at both the sender and receiver. Due to the presence of a number of antennas, mutual coupling predominates. Several methods, including neutralization line [4–7], parasitic elements [8–10], defected ground structures [11], decoupling structures [12–15], and stubs [16] have been suggested to reduce interference between entities. The primary challenge in designing UWB antennas is the potential for interference from narrow band systems, which arises from the need to share frequency bands. Various narrow band systems like WiMAX (3.2–3.8 GHz), C-band (3.7–4.2/5.9–6.4 GHz), INSAT (4.4–4.9 GHz), WLAN (5.1–5.8 GHz), X-band (7.7–8.4 GHz) also exist in UWB. Putting band reject filters at the antenna system's output is one way to get rid of these frequencies. However, this will increase the antenna system's intricacy. Therefore, it is difficult to achieve notch characteristics while keeping implementation intricacy to a minimum. To overcome the problem of interference from different frequencies, it is crucial to use an antenna that can reject signals across multiple bands. Several researchers have put forward various techniques to create antennas that can suppress signals in one, two, or three frequency bands. A multiple input multiple output antenna that consists of dual quasi-self-complementary (QSC) antennas for the mitigation of WLAN frequency is designed with the help of slits on each antenna [17]. Researchers have proposed a miniaturized octagonal type UWB-MIMO antenna

Received 30 December 2022, Accepted 14 March 2023, Scheduled 29 March 2023

* Corresponding author: Sadineni Ramesh Babu (srameshbabu@rvrjc.ac.in).

[1] Department of ECE, RVR&JC College of Engineering, Guntur 522019, India. [2] Department of ECE, Dayananda Sagar College of Engineering, Bengaluru 560078, India.

for the suppression of WLAN narrow band by employing a C-type slot on the antenna along with increased isolation in [18]. A miniature MIMO antenna with band-stop filter on the ground for increase in isolation has been explored in [19]. In [20], a MIMO antenna is introduced that has high isolation and uses a stepped stub as a decoupling mechanism, while also possessing the ability to reject signals in specific frequency bands. [21] discusses a distinctive UWB-MIMO Vivaldi antenna that features increased element separation and a single notch characteristic, made possible by incorporating a T-shaped slot above the ground and two strategically placed SRRs. [22] examines a dual-port miniaturized UWB-MIMO antenna that is capable of creating notches in two frequency bands by using slots and a T-shaped stub in its design. [23] investigates a UWB antenna that has been enhanced with a slot and an electromagnetic band. In [24–30], various small size UWB-MIMO antennas with enhanced isolation and triple band & penta band mitigation features are implemented. In [31], a two element UWB MIMO antenna of size $40 \times 40\,\text{mm}^2$ with four notches is demonstrated. A compact polarization diversity quadruple band notch UWB MIMO antenna is described in [32]. An electromagnetic band gap (EBG) based quadruple band notch UWB-MIMO antenna is explored in [33]. In [34, 35], various compact UWB-MIMO antennas are analyzed with dual band notch characteristics.

To effectively reduce interference to a negligible level, it is crucial to abolish any significant intrusive bands that fall within the UWB. The current literature on UWB antenna designs focuses mainly on techniques to suppress single, dual, and triple band notches, with very limited coverage of methods to reject quadruple bands. Additionally, UWB antenna designs discussed in the current literature are massive in size and not suitable for the use in portable systems. Therefore, this article suggests a MIMO antenna design with strong isolation that can suppress four frequency bands in the ultra-wideband range, making it suitable for various wireless applications. The reported design offers a novel feature of achieving a greater number of notches within UWB, while allowing for sharpness control of the rejections. Additionally, the design ensures better isolation of less than $-25\,\text{dB}$ across the necessary resonating bandwidth for MIMO systems.

2. ANTENNA DESIGN AND ANALYSIS

2.1. Design Approach for Achieving UWB Characteristics

The design process for the ultra-wide band antenna is illustrated in Figure 1. The reported antenna is constructed using copper and lithographed on an FR-4 lossy substrate that is $20 \times 24 \times 1.6\,\text{mm}^3$ in size, with a permittivity of 4.3, thickness of 1.6 mm, and loss tangent of 0.02. The copper foil has a thickness of 0.035 mm and a conductance of 5.8e+007 S/m. Initially, a rectangular radiator is placed above the substrate with reduced ground (Ant#1) as shown in Figure 1(a). However, this configuration causes a irregularity in the feed line connection that results in current concentration at the lower corners of the antenna, reducing radiation effectiveness at higher frequencies. To overcome this issue, Antenna#2 is proposed by adding two rounded slots at the ground's top corners and a groove at the center, as well as tapering the lower corners of the patch to increase impedance bandwidth. As shown in Figure 2(c), Antenna#2 operates within the required frequency range for UWB systems, extending from 2.9 to 12 GHz.

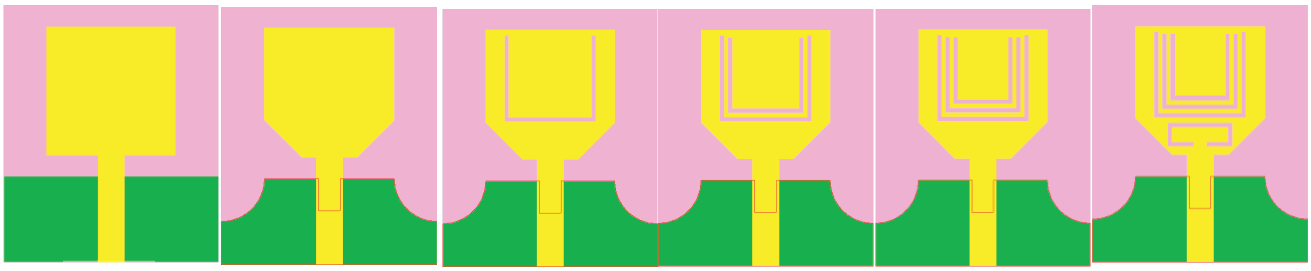

Figure 1. Evolution steps of the reported Quadruple band reject UWB antenna. (a) Ant#1. (b) Ant#2. (c) Ant#3. (d) Ant#4. (e) Ant#5. (f) Ant#6.

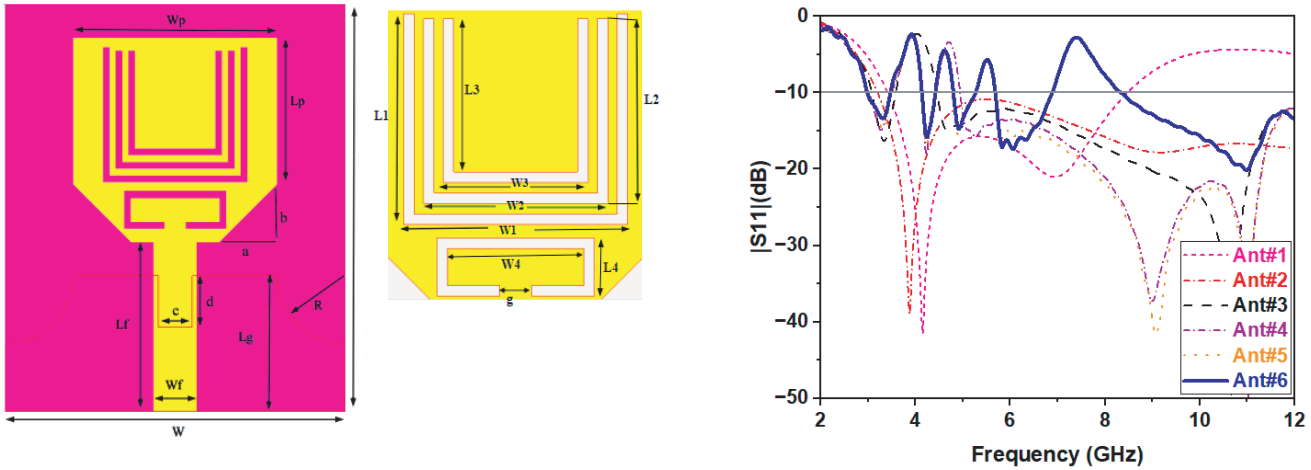

(a) (b) (c)

Figure 2. (a) Suggested band reject UWB antenna. (b) Slots. (c) Return loss characteristics.

Narrow band systems such as 5G, INSAT, WLAN, and X-band also operate within the UWB frequency range and can cause interference due to spectrum sharing. To address this intrusion, numerous notch techniques, such as creation of slots, have to be included in UWB antenna design after analyzing its characteristics. Figures 2(a) & (b) depict a quad-band reject UWB antenna with three U-shape slots and a split ring resonator, which effectively suppress intrusion from 5G, INSAT, WLAN, and X-bands. The outer U-shaped slot produces a notch at 3.9 GHz; the middle U-shape slot generates a notch at 4.6 GHz; and the inner U-shape slot creates a notch at 5.5 GHz. Additionally, an SRR is etched to generate a notch at 7.4 GHz. The length of each slot is computed by a formula.

$$f_n^i = \frac{co}{2L_{slot}^i\sqrt{\varepsilon_{eff}}} \tag{1}$$

$$L_{slot}^i = 2L_i + W_i \tag{2}$$

$$\varepsilon_{eff} = \frac{\varepsilon_r + 1}{2} \tag{3}$$

where C is the velocity of light in free space, and ε_{eff} is the effective dielectric constant of the substrate.

The UWB antenna in Figure 2(a) was designed using CST MW Studio 2018, based on calculated dimensions for the quadruple band notch antenna which were determined as follows: $L = 24$, $W = 20$, $Lp = 12$, $Wp = 12$, $Wg = 20$, $Lg = 8.5$, $Wf = 2.5$, $Lf = 10$, $L1 = 8$, $L2 = 7$, $L3 = 6.2$, $L4 = 2.2$, $W1 = 8.5$, $W2 = 7$, $W3 = 5.5$, $W4 = 6$, $a = 2$, $b = 2$, $c = 2$, $d = 3$, $R = 3.8$, $g = 1.2$. All dimensions are in mm.

2.2. Parametric Analysis

Figure 3 provides a visual depiction and explanation of the return loss characteristics that can be compared to better comprehend how the rejection process is controlled with precision. S-parameters for each notch band, generated by altering the dimensions of the corresponding band notch structure, are displayed in the figure. The key parameters for achieving the notch band characteristics with respect to U-shaped slots and SRR slot are $L1$, $L2$, $L3$, $L4$, $W1$, $W2$, $W3$, and $W4$. These parameters are essential since the currents that flow through U-shape slots travel in opposite directions at specific frequencies, which contributes to the characteristics of the notch band.

To optimize the design, only one parameter is adjusted at a time while the other design factors are maintained constant for each individual notch element. The S_{11} (dB) plots for the quadruple band suppressed UWB antenna are shown in Figures 3(a)–(d). The figures indicate that when the length of the notching structure is increased, the target frequency range where the signal is blocked is also shifted

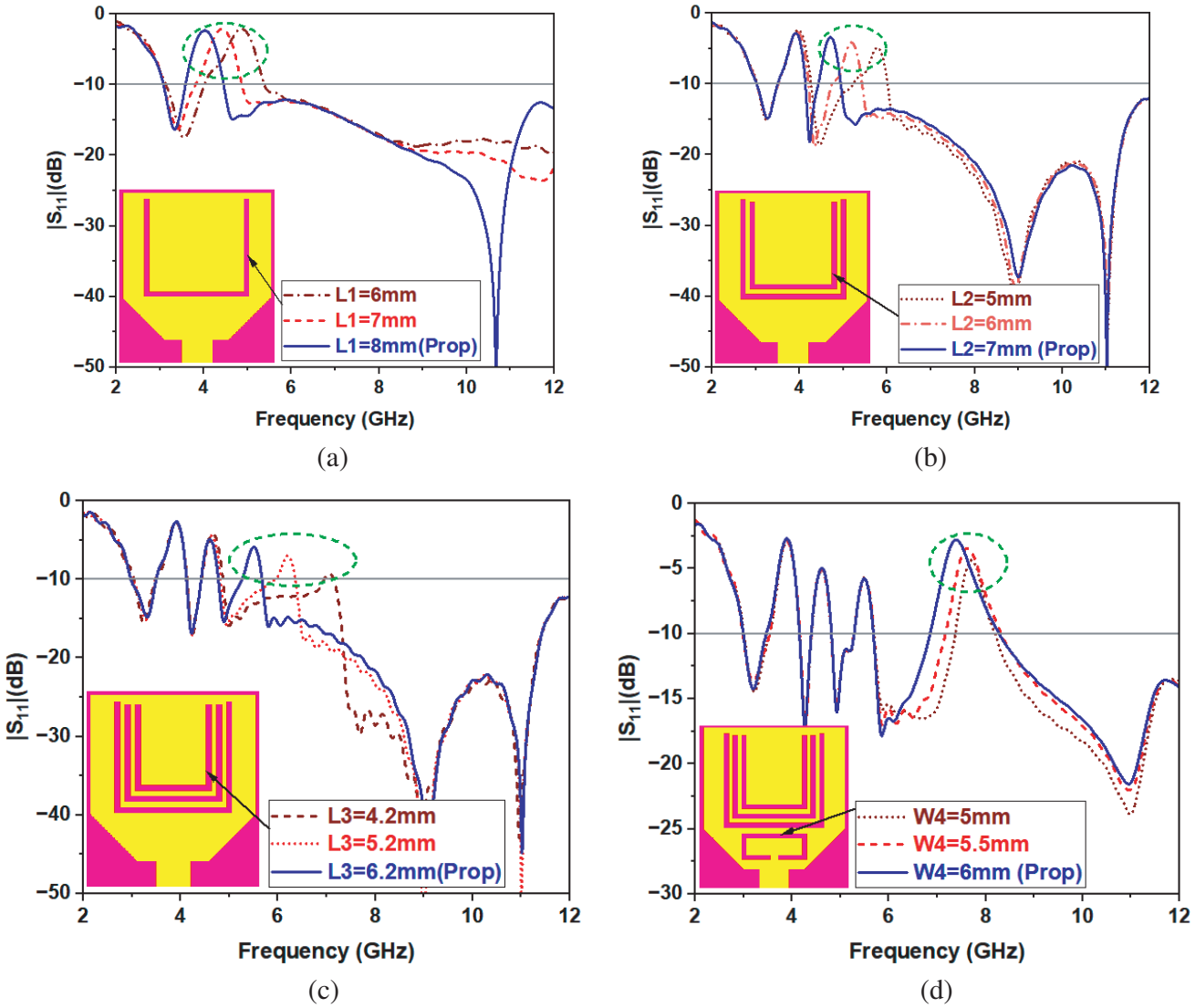

Figure 3. Simulated S_{11} plot for variation in (a) length of outer slot ($L1$), (b) length of middle slot ($L2$), (c) length of inner slot ($L3$), (d) width of SRR slot ($W4$).

towards the lower end of the frequency band. On the other hand, a short length notching structure shifts the target stopband towards high frequency end. Equations (1)–(3) illustrate that there is an inverse relationship between the total length of the notching structure and the frequency at which the signal is intended to be blocked. Moreover, it is demonstrated that the notch frequencies are essentially unrelated to each other. Therefore, by making appropriate changes to the sizes and locations of the relevant components that control the frequency band and notches, it is possible to achieve the desired notch frequency and bandwidth.

3. DESIGN OF PROPOSED TWO-PORT ULTRA WIDE BAND MIMO ANTENNA

The design layout of dual port UWB MIMO antenna is shown in Figure 4. Initially, two antenna elements are placed in a collinear manner, as depicted in Figure 4(a). The footprint of the proposed collinear antenna is only $24 \times 40 \times 1.6\,\text{mm}^3$.

In Figure 4(b), the simulated and measured S-parameters (S_{11} and S_{12}) of the proposed dual port collinear UWB-MIMO antenna are shown. The simulation results indicate that the antenna achieves

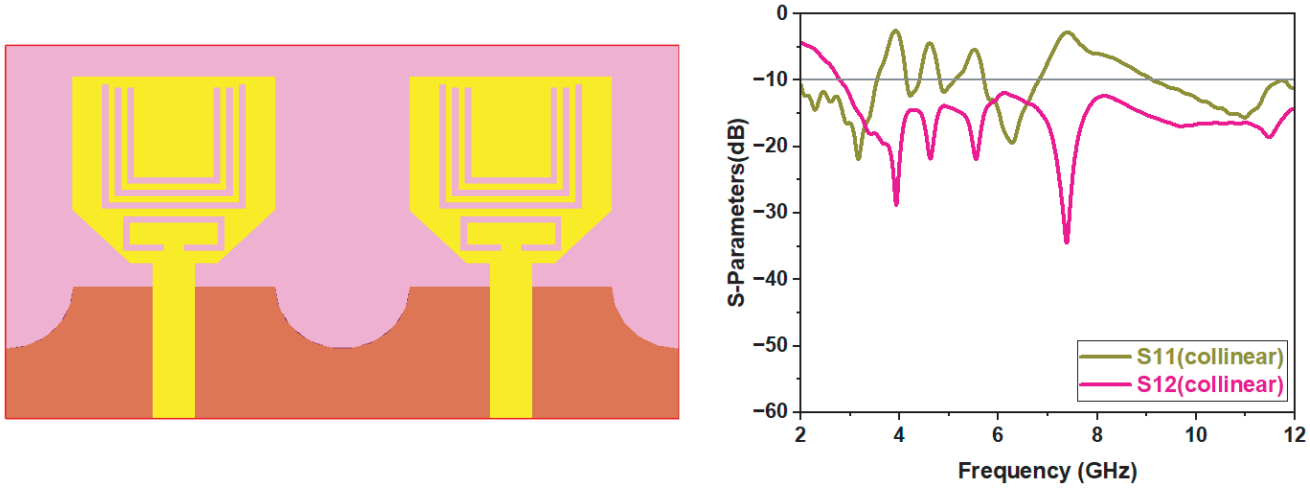

(a) (b)

Figure 4. (a) Collinear UWB-MIMO antenna. (b) Variation of S_{11} & S_{12}.

the desired four notches within the UWB. However, the isolation between the antenna structures is only below −10 dB, which is not sufficient for a MIMO antenna in a mobile scenario where the isolation has to be less than −20 dB.

To further improve the isolation between the two antenna elements, they are positioned perpendicular to each other as illustrated in Figure 5(a). This configuration results in better isolation between the antenna structures, which enables polarization diversity to be achieved with an isolation of smaller than −25 dB over the entire operating bandwidth which is shown in Figure 5(b). Figures 5(c) & (d) show the measured S-parameters. Photographs of the fabricated antenna are shown in Figures 5(e) & (f). The analysis suggests that polarization diversity is more effective than spatial diversity in reducing mutual coupling. The orthogonal arrangement of the antenna elements is found to provide a spatial diversity performance of −12 dB.

4. RESULTS AND DISCUSSION

Figure 6 presents current distribution of the proposed antenna, which helps understand how the notched band phenomenon is achieved. When port-1 is turned on and the other port turned off, the areas with the highest current concentrations are located on the outer edge of the slot at 3.86 GHz, in the middle of the slot at 4.6 GHz, in the inner slot at 5.51 GHz, and in the SRR slot at 7.41 GHz. These areas of high current concentration are not present in other parts of the antenna array. The arrangement of the band-notches causes the currents to flow in opposite directions along the edges that move away from each other, thereby eliminating the radiation fields. As a result of the above phenomenon, each band-notch arrangement functions as a non-radiating structure when the frequency corresponds to the band-notch frequency.

Figure 7 illustrates the simulated and measured radiation patterns in the E-plane and H-plane for the reported UWB-MIMO antenna. The radiation patterns are presented for two resonant frequencies of 4.17 GHz and 4.91 GHz, respectively.

Figure 7 presents the radiation patterns of the UWB-MIMO antenna in both E-plane and H-plane, which show directional radiation in the E-plane and semi-omnidirectional radiation in the H-plane for two resonant frequencies (4.17 GHz and 4.91 GHz). In addition, Figure 8(a) shows the simulated and measured gains of the antenna, which are almost consistent across the operating bandwidth except for a decrease at the four notch frequencies, indicating successful blocking of interference from 5G, INSAT, WLAN, and X-band systems.

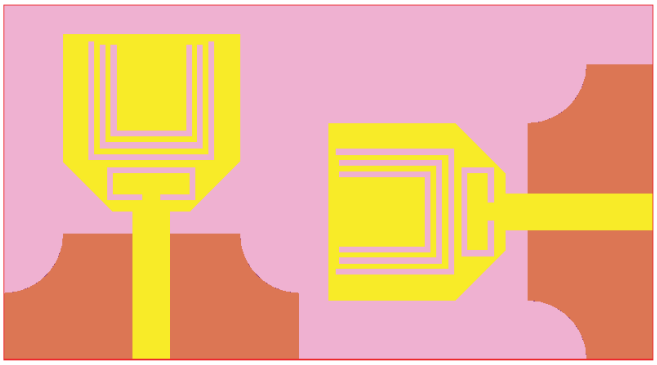

(a)

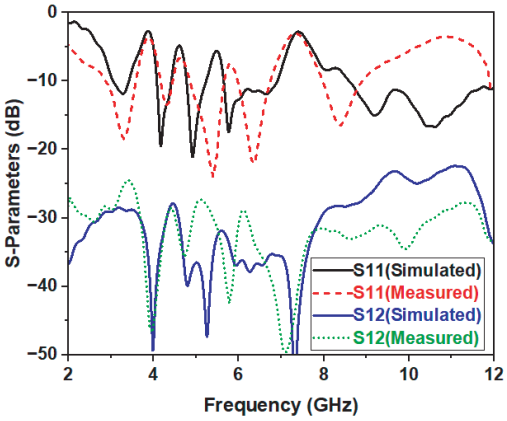

(b)

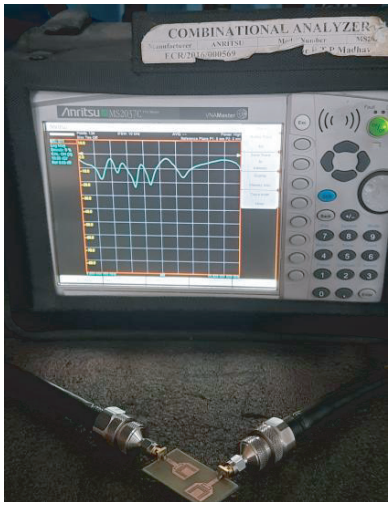

(c)

(d)

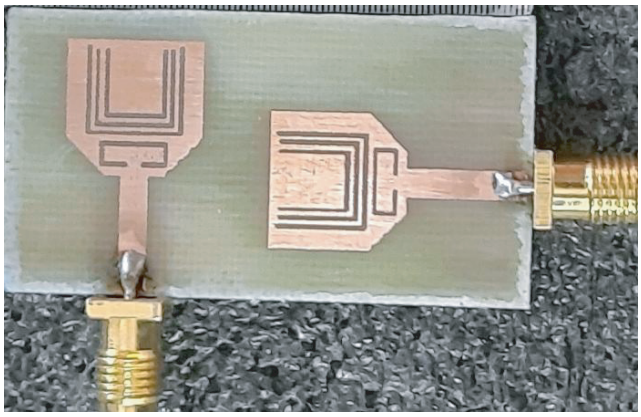

(e)

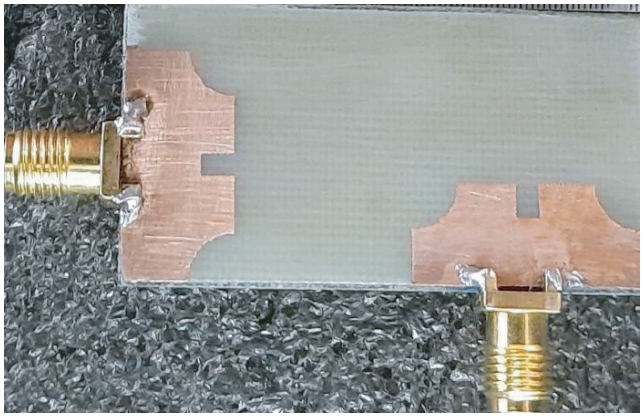

(f)

Figure 5. (a) Two element orthogonal UWB-MIMO antenna. (b) Variation of S_{11} & S_{12}. (c) Photograph taken during measurement of S_{11} using Vector Network analyzer. (d) Photograph taken during measurement of S_{12} using Vector Network analyzer. (e) Fabricated prototype model (Top-view). (f) Fabricated prototype mode (Bottom-view).

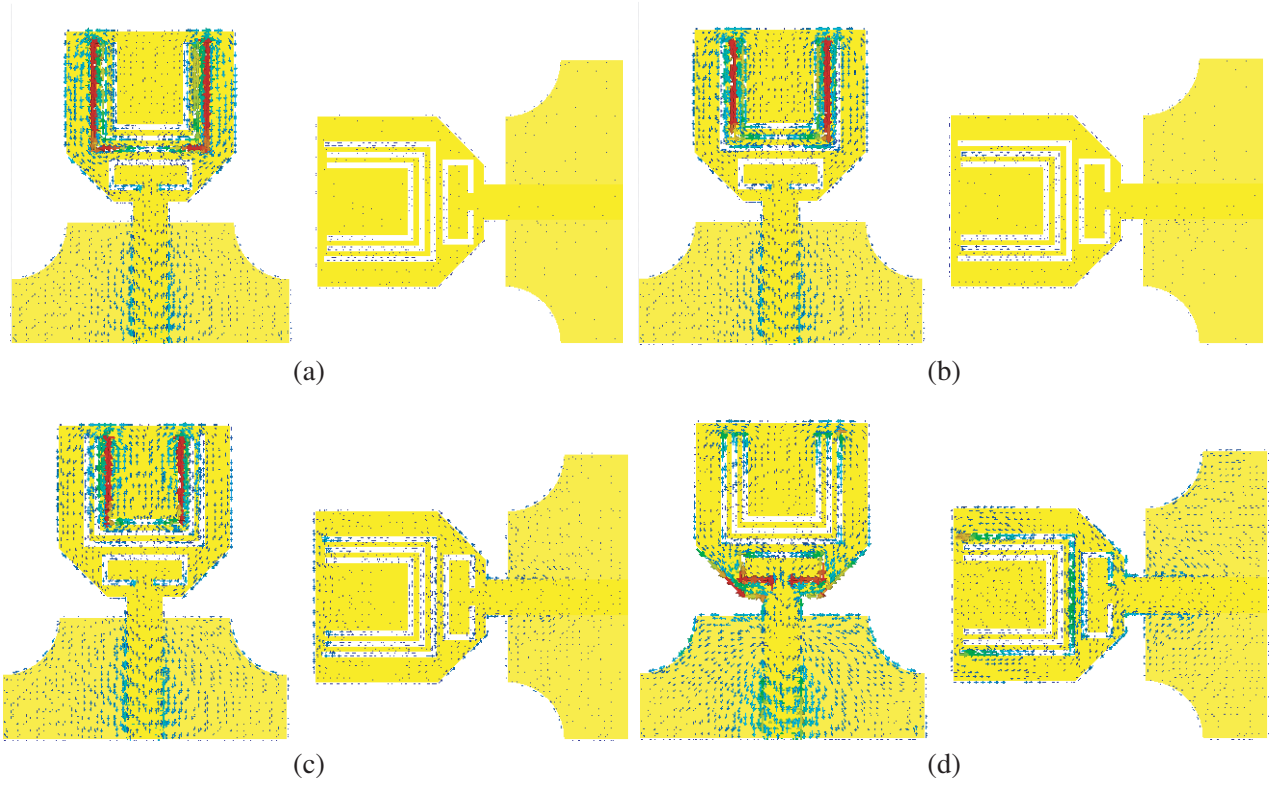

Figure 6. Surface current distribution for the reported dual port UWB-MIMO antenna. (a) 3.86 GHz. (b) 4.6 GHz. (c) 5.51 GHz. (d) 7.41 GHz.

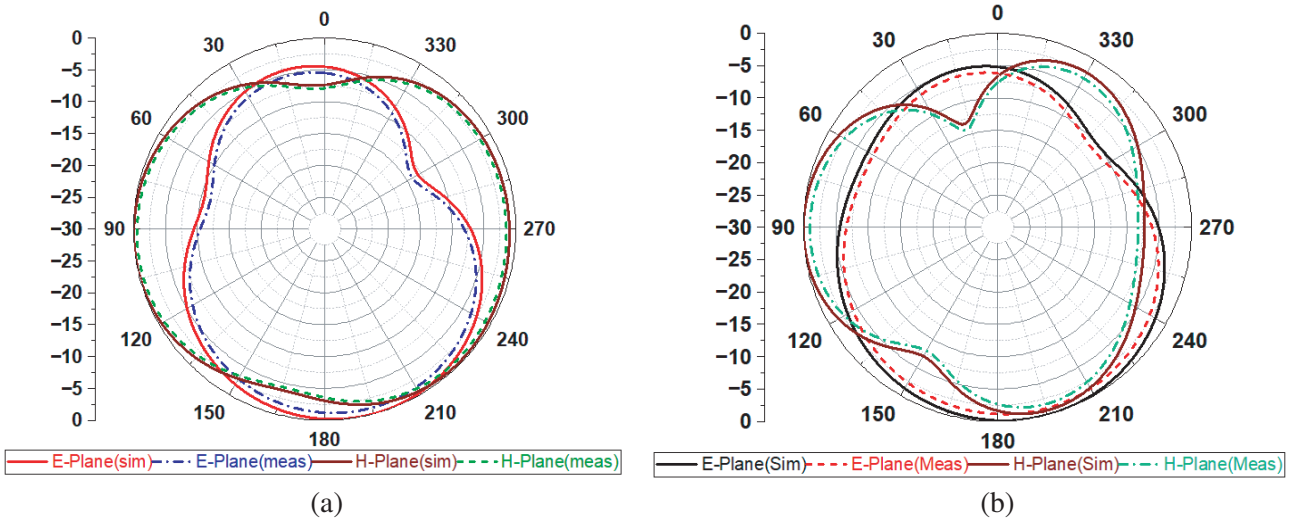

Figure 7. Normalized radiation characteristics at (a) 4.17 GHz, (b) 4.91 GHz.

4.1. Time Domain Characteristics

Ultra-wideband technology relies on quick bursts of energy to send and receive information. The signal may be distorted and spread out because of the transmission channel and the distance. Therefore, UWB antenna necessitates more thorough parameter analysis than regular antennas. For this time-domain study, we place two matching antennas 100 mm apart in both a face-to-face and a side-by-side arrangement. As shown in Figure 8(b), group delay is less than 1 ns except at notch frequencies.

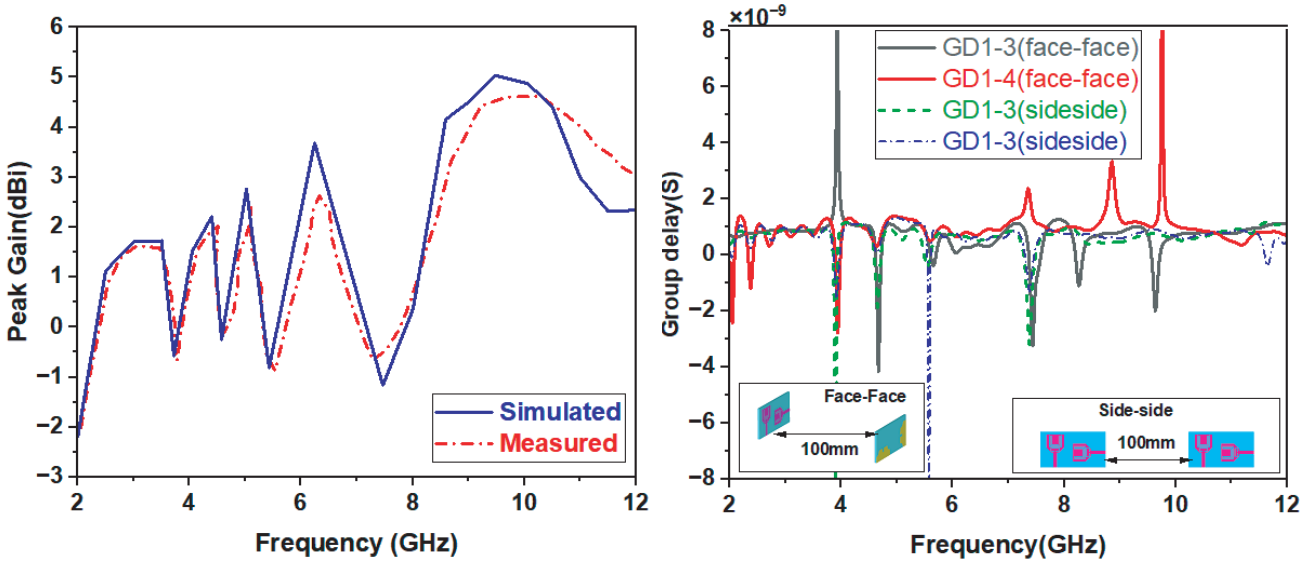

Figure 8. (a) Gain versus frequency. (b) Group delay of the suggested antenna in various configurations.

4.2. Diversity Characteristics

In this section, the effectiveness of the reported UWB-MIMO antenna is examined in a multi-path fading scenario using various diversity performance measures such as envelope correlation coefficient and diversity gain.

4.3. Envelope Correlation Coefficient

This section discusses the importance of the envelope correlation coefficient (ECC) as a diversity parameter for evaluating the interference between adjacent antennas in a MIMO array. The ECC takes into account the effect of S-parameters on the behavior of the array, and for reliable operation in fading environment, the ECC must be less than 0.5. The ECC can be calculated using the S-parameters of the MIMO antenna, as given in Equation 4. Reference [30] is cited as the source for this information.

$$ECC = \frac{|S_{ii} * S_{ij} + S_{ji} * S_{jj}|^2}{\left(1 - |S_{ii}|^2 - S_{ij}^2\right)\left(1 - |S_{ji}|^2 - S_{jj}^2\right)} \tag{4}$$

4.4. Diversity Gain

The diversity gain (DG) is a crucial metric that measures the improvement in the signal-to-noise ratio (SNR) achieved by utilizing diversity techniques in a MIMO antenna system. A higher DG implies better reception quality in a fading channel. ECC and DG are correlated with each other as depicted in Equation (5).

$$DG = 10\sqrt{1 - ECC^2} \tag{5}$$

The simulation results depicted in Figure 9(a) demonstrate that envelope correlation coefficient (ECC) and diversity gain (DG) are below 0.05 and around 10 dB, respectively, across the entire operating frequency range of the reported UWB-MIMO antenna, except for the notched frequencies. This indicates that the reported UWB-MIMO antenna exhibits outstanding diversity performance.

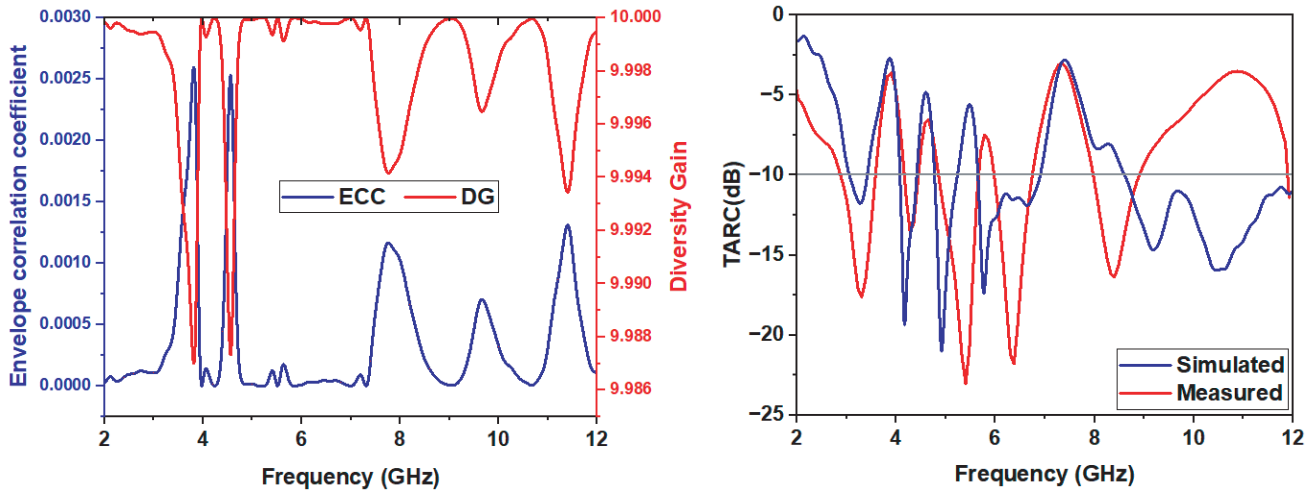

(a) (b)

Figure 9. (a) ECC and DG. (b) TARC.

4.5. Total Active Reflection Coefficient

Total active reflection coefficient (TARC) is a vital diversity parameter for characterizing MIMO performance as a function of impedance bandwidth and resonant frequency. It is the ratio of square root of whole reflected power to incident power in the overall MIMO antenna system. TARC can be evaluated as

$$TARC = \frac{\sqrt{\sum_{i=1}^{4}\left|S_{i1} + \sum_{n=2}^{4} S_{in}e^{j\theta_{n-1}}\right|^2}}{2} \tag{6}$$

The antenna's total active reflection coefficient (TARC) is shown in Figure 9(b), which indicates that TARC values are lower than −10 dB over the operating frequency range, except for the notch frequencies. Furthermore, the performance of the suggested antenna is evaluated by comparing it with the outcomes of previously published studies on band reject antennas for UWB, and the findings are summarized in Table 1.

Table 1. Performance comparison with state of art models.

Ref./Year	Size (mm)	Operating BW	No. of notches	Gain	Isolation (dB)	ECC
[2]/2013	26 × 40	2.9–10.6	NA	6.5	−15	< 0.2
[19]/2015	45 × 45	2–10.6	1	4	−17	< 0.01
[21]/2017	30 × 30	3.1–11	1	5	−20	< 0.02
[23]/2020	19 × 30	3.1–10.6	2	1.2–2.91	−18	< 0.13
[26]/2018	64 × 45	2.5–11	3	6	−15	< 0.02
[33]/2021	43 × 34.9	3–10.7	4	6	−25	< 0.05
[34]/2022	21.5 × 28	3.4–11.9	2	5	−16	< 0.3
[35]/2022	44 × 44	2.4–12.4	2	5	−15	< 0.3
Proposed	**24 × 40**	**2.9–12**	**4**	**5**	**−25**	**< 0.003**

5. CONCLUSION

This article presents a study on a dual port ultra-wideband multiple-input multiple-output antenna with quad-band notch characteristics. The reported antenna is designed with two compact rectangular patch antenna elements arranged in an orthogonal pattern, providing better isolation among antenna ports. The radiators feature three U-shape slots and a split ring resonator to suppress intrusion from 5G, INSAT, WLAN, and X-band. The proposed antenna demonstrates band rejection at the intended notch frequencies, and the surface current variation validates this principle. The broad band gain ranges from -0.75 dB to 5 dB, with minimal values at the notch frequencies. The reported antenna provides good diversity performance such as low ECC (< 0.003) and high DG (≥ 9.99) for receiving diversity techniques across the resonating bandwidth except at notches.

REFERENCES

1. "Federal Communications Commission: Revision of Part 15 of the Commission's Rules Regarding Ultra-Wideband Transmission System from 3.1 to 10.6 GHz," *Federal Communications Commission*, 98–153, ET-Docket, Washington, DC, 2002.
2. Liu, L., S. W. Cheung, and T. I. Yuk, "Compact MIMO antenna for portable devices in UWB applications," *IEEE Transactions on Antennas and Propagation*, Vol. 61, No. 8, 4257–4264, 2013.
3. Li, Z., C. Yin, and X. Zhu, "Compact UWB MIMO Vivaldi antenna with dual band-notched characteristics," *IEEE Access*, Vol. 7, 38696–38701, 2019.
4. Zhang, S. and G. F. Pedersen, "Mutual coupling reduction for UWB MIMO antennas with a wideband neutralization line," *IEEE Antennas and Wireless Propagation Letters*, Vol. 15, 166–169, 2016.
5. Su, S.-W., C.-T. Lee, and F.-S. Chang, "Printed MIMO-antenna system using neutralization-line technique for wireless USB-dongle applications," *IEEE Transactions on Antennas and Propagation*, Vol. 60, No. 2, 456–463, Feb. 2012.
6. Vasu Babu, K. and B. Anuradha, "Design of Wang shape neutralization line antenna to reduce the mutual coupling in MIMO antennas," *Analog. Integr. Circ. Sig. Process.*, Vol. 101, 67–76, 2019.
7. Sun, Y., M. Tian, and G. S. Cheng, "Characteristics mode based neutralization line design for MIMO antenna," *International Journal of Antennas and Propagation*, Vol. 2022, 1–14, 2022.
8. Quevedo-Teruel, O., L. Inclan-Sanchez, and E. Rajo-Iglesias, "Soft surfaces for reducing mutual coupling between loaded PIFA antennas," *IEEE Antennas and Wireless Propagation Letters*, Vol. 9, 91–94, 2010.
9. Zuo, S., Y.-Z. Yin, W.-J. Wu, Z.-Y. Zhang, and J. Ma, "Investigations of reduction of mutual coupling between two planar monopoles using two $\lambda/4$ slots," *Progress In Electromagnetics Research Letters*, Vol. 19, 9–18, 2010.
10. Wang, H., D. G. Fang, and X. L. Wang, "Mutual coupling reduction between two microstrip patch antennas by using the parasitic elements," *Asia-Pacific Microwave Conference*, Vol. 2008, 1–4, 2008.
11. Acharjee, J., K. Mandal, and S. K. Mandal, "Reduction of mutual coupling and cross-polarization of a MIMO/diversity antenna using a string of H-shaped DGS," *International journal of Electronics and communications*, Vol. 97, 110–119, 2018.
12. Radhi, A., R. Nilavalan, Y. Wang, H. Al-Raweshidy, A. Eltokhy, and N. Ab Aziz, "Mutual coupling reduction with a wideband planar decoupling structure for UWB-MIMO antennas," *International Journal of Microwave and Wireless Technologies*, Vol. 10, No. 10, 1143–1154, 2018.
13. Babu, J. K., W. R. Aldhaheri, Y. M. Talha, and S. I. Alruhaili, "Design of a compact two element MIMO antenna system with improved isolation," *Progress In Electromagnetics Research Letters*, Vol. 48, 27–32, 2014.
14. Lee, Y., D. Ga, and J. Choi, "Design of a MIMO antenna with improved isolation using MNG metamaterial," *International Journal of Antennas and Propagation*, Vol. 2012, 1–7, 2012.

15. Khan, M. K., Q. Feng, and Z. Zheng, "Experimental investigation and design of UWB MIMO antenna with enhanced isolation," *Progress In Electromagnetics Research C*, Vol.107, 287–297, 2021.
16. Altaf, A., A. Iqbal, A. Smida, J. Smida, A. A. Althuwayb, S. Hassan Kiani, M. Alibakhshikenari, F. Falcone, and E. Limiti, "Isolation improvement in UWB-MIMO antenna system using slotted stub," *Electronics*, Vol. 9, No. 10, 1582, 2020.
17. Iqbal, A., O. A. Saraereh, A. W. Ahmad, and S. Bashir, "Mutual coupling reduction using F-shaped stubs in UWB-MIMO antenna," *IEEE Access*, Vol. 6, 2755–2799, 2018.
18. Zhu, J., S. Li, B. Feng, L. Deng, and S. Yin, "Compact dual-polarized UWB quasi-self-complementary MIMO/diversity antenna with band-rejection capability," *IEEE Antennas and Wireless Propagation Letters*, Vol. 15, 905–908, 2016.
19. Tripathi, S., A. Mohan, and S. Yadav, "A compact koch fractal UWB MIMO antenna with WLAN band-rejection," *IEEE Antennas and Wireless Propagation Letters*, Vol. 14, 1565–1568, 2015.
20. Khan, M. S., B. D. Braaten, A. Iftikhar, A. D. Capobianco, B. Ijaz, and S. Asif, "Compact 4×4 UWB-MIMO antenna with WLAN band rejected operation," *Electronics Letters*, Vol. 51, 1048–1050, 2015.
21. Biswal, P. and S. Das, "A low-profile dual port UWB-MIMO/diversity antenna with band rejection ability," *International Journal of RF and Microwave Computer Aided Engineering*, Vol. 28, No. 1, 2017.
22. Li, Z., C. Yin, and X. Zhu, "Compact UWB MIMO vivaldi antenna with dual band-notched characteristics," *IEEE Access*, Vol. 7, 38696–38701, 2019.
23. Kumar, A., Q. A. Ansari, K. B. Kanaujia, J. Kishor, and S. Kumar, "An ultra compact two-port UWB MIMO antenna with dual band notched characteristics," *AEU — International Journal of Electronics and Communications*, Vol. 114, 1–12, 2020.
24. Kadam, A. A. and A. A. Deshmukh, "Pentagonal shaped UWB antenna loaded with slot and EBG structure for dual band notched response," *Progress In Electromagnetics Research M*, Vol. 95, 165–176, 2020.
25. Tang, Z., X. Wu, J. Zhan, S. Hu, Z. Xi, and Y. Liu, "Compact UWB-MIMO antenna with high isolation and triple band-notched characteristics," *IEEE Access*, Vol. 7, 19856–19865, 2019.
26. Jaglan, N., S. D. Gupta, E. Thakur, D. Kumar, B. K. Kanaujia, and S. Srivastava, "Triple band notched mushroom and uniplanar EBG structures based UWB MIMO/diversity antenna with enhanced wide band isolation," *AEU — International Journal of Electronics and Communications*, Vol. 90, 36–44, 2018.
27. Doddipalli, S. and A. Kothari, "Compact UWB antenna with integrated triple notch bands for WBAN applications," *IEEE Access*, Vol. 7, 183–190, 2019.
28. Chen, Z., W. Zhou, and Z. Hong, "A miniaturized MIMO antenna with triple band-notched characteristics for UWB applications," *IEEE Access*, Vol. 9, 63646–63655, 2021.
29. Kumar, P., S. Urooj, and F. Alrowais, "Design of quad-port MIMO/diversity antenna with triple-band elimination characteristics for super-wide band applications," *Sensors*, Vol. 20, 1–12, 2020.
30. Sadineni, R. B. and P. G. Dinesha, "Design of penta-band notched UWB MIMO antenna for diverse wireless applications," *Progress In Electromagnetics Research M*, Vol. 107, 35–49, 2022.
31. Yu, K., Y. Kong, and Y. Li, "A two-element UWB-MIMO antenna with quad narrowband frequency rejection characteristics," *2016 IEEE/ACES International Conference on Wireless Information Technology and Systems (ICWITS) and Applied Computational Electromagnetics (ACES)*, 1–2, Honolulu, HI, USA, 2016.
32. Cai, X. and L. Jin, "Compact polarization diversity ultra-wideband MIMO antenna with quadruple band-notched characteristics," *2016 IEEE 13th International Conference on Signal Processing (ICSP)*, 1566–1570, Chengdu, China, 2016.
33. Sumon, M. and K. Taimoor, "A slotted UWB-MIMO antenna with quadruple band-notch characteristics using mushroom EBG structure," *AEU — International Journal of Electronics and Communications*, Vol. 134, 153673, 2021.

34. Kumar, P., T. Ali, and M. P. Mm, "Characteristic mode analysis-based compact dual band-notched UWB MIMO antenna loaded with neutralization line," *Micromachines*, Vol. 13, 1599, 2022.
35. Mukherjee, S., A. Roy, S. Maity, T. Tewary, P. Sarkar, and S. Bhunia, "Design of dual band-notched UWB hexagonal printed microstrip antenna," *International Journal of Microwave and Wireless Technologies*, 1–9, 2022.